Journal of Power Sources 196 (2011) 1620–1625

Contents lists available at ScienceDirect

Journal of Power Sources

journal homepage: www.elsevier.com/locate/jpowsour

Spark plasma sintered carbon electrodes for electrical double layer capacitor applications

B. Daffos, G. Chevallier, C. Estournès, P. Simon*

Université Paul Sabatier de Toulouse, CIRIMAT UMR CNRS 5085, 118 Route de Narbonne, 31062 Toulouse Cedex, France

ARTICLE INFO

Article history:
Received 27 May 2010
Received in revised form 22 July 2010
Accepted 29 August 2010
Available online 6 September 2010

Key words:
Spark plasma sintering
Microporous carbon
Supercapacitors
Energy storage

ABSTRACT

The spark plasma sintering (SPS) is an emerging process for shaping any type of materials (metals, ceramic, polymers and their composites). The advantage of such a process is to prepare densified ceramic materials in a very short time, while keeping the materials internal porosity. In the present work, we have used the SPS technique to prepare activated carbon-based electrodes for Electrochemical Double Layer Capacitor applications (EDLC). Self-supported 600 and 300 μm-thick electrodes were prepared and characterized using of Electrochemical Impedance Spectroscopy and galvanostatic cycling in a non-aqueous 1.5 M NEt_4BF_4 in acetonitrile electrolyte. Electrochemical performance of these sintered electrodes were found to be in the same range – or even slightly better – than the conventional tape-casted activated carbon electrodes. Although organic liquid electrolyte was used to characterize the electrochemical performance of the sintered electrodes, these results demonstrate that the SPS technique could be worth of interest in the ultimate goal of designing solid-state supercapacitors.

1. Introduction

Electrochemical capacitors (ECs), also named as supercapacitors, are electrochemical energy storage devices which fill the gap between batteries and dielectric capacitors because of their capability to deliver high power during few seconds [1–4]. ECs are used in various applications, most of them needing small capacitance cells (<100 F), like power buffer or power delivery for short time. Large-capacitance cells (>100 F) are mainly used in transportation applications such as tramways, buses or planes [2,4], where they can nicely complement Li-ion batteries. One of the main interests of ECs vs batteries is their fast charge rate capability, which is useful for energy harvesting. Electrochemical Double Layer Capacitors, which store the charge through the reversible adsorption of ions from the electrolyte at high surface area carbons, are constituted by two symmetrical electrodes separated by a porous separator soaked with a liquid electrolyte. Electrodes are usually prepared following a wet route, by casting a mixture of active material (high surface area carbon) with an electronic conductor (Carbon Black) and a binder (PVDF or PTFE for instance) onto a current collector foil or grid (Al). Although this process is well-adapted for manufacturing large capacitance devices, it could be interesting to propose alternative processing routes for small devices, dedicated to power electronics applications. For instance, using a high temperature sintering process to prepare an all solid-state supercapacitor would allow their direct integration onto a Printed Circuit Board substrate (PCB) by being compatible with the solder reflow process [5]. Additionally, high surface area sintered carbon electrodes may offer a lower resistivity by improving the contacts between the carbon grains, which would have a positive impact onto the power capability of the EDLC.

Conventional sintering processes consist in a thermal treatment of powders at high temperature and pressure for finally obtaining the densified material (ceramic). Because EDLCs electrodes use high surface area porous carbon powders as active material, this process would led to the destruction of the porous structure of the carbon grains by densification, thus leading to very poor capacitive behavior. Recently, a new sintering technique was proposed for batteries and dielectrics materials synthesis: the spark plasma sintering (SPS). SPS is a flash, short time, sintering technique [6,7] that allows shaping various materials from powders (metals and alloys, ceramic, polymers and their composites) [8–13]. The advantage of this technique is to obtain in a very short time highly-densified materials from powders with controlled grain growth, without any change of chemical composition or porosity, thus confering to these materials unusual properties [14]. For batteries, in particular for lithium-ion batteries, it was recently demonstrated that the densification of the solid LIPON electrolyte significantly increased its ionic conductivity [15,16]. Following this work, successful attempts have been reported to prepare all solid-state Li-ion battery for high temperature applications [17]. For dielectric capacitors, materials with outstanding permittivity val-

* Corresponding author. Tel.: +33 5 61 55 68 02; fax: +33 5 61 55 61 63.
E-mail address: simon@chimie.ups-tlse.fr (P. Simon).

0378-7753/$ – see front matter © 2010 Elsevier B.V. All rights reserved.
doi:10.1016/j.jpowsour.2010.08.098

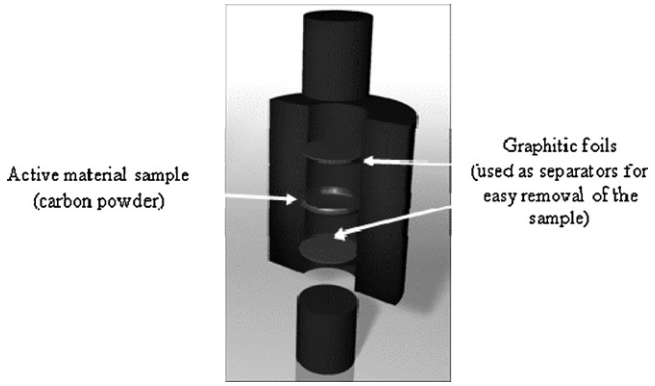

Fig. 1. Schematic drawing of SPS die.

ues were prepared by controlling the flash sintering parameters [18,19].

This paper reports the first results of the use of the SPS technique in the ultimate goal of preparing a solid-state EDLC. We focus here on the self-supported sintered electrode preparation from high surface area carbon powder. Activated carbon powders have been processed into sintered plates and the structural and electrochemical properties of these electrodes are reported.

2. Experimental

2.1. Preparation of active material films and sintering process

The sintered electrodes were made using a two-step process:

(i) Following the conventional formulation of active materials previously described [20], activated carbon powder (Arkema Company) and PolyTetraFluoroEthylene (PTFE) binder in suspension in aqueous electrolyte (Dupont de Nemours) were mixed together. Ethanol was then added to the solution under vigorous magnetic stirring, and the solvent was evaporated by heating at 80 °C. The ink obtained was processed into films of various thicknesses by canlendering (between 300 and 600 μm).

(ii) The second step is the active material film sintering under dynamic vacuum (0.05 mBar) to prepare the self-supported solid-state electrodes. All samples were sintered using a Dr Sinter 2080 SPS apparatus (SPS Syntex Inc., Tokyo, Japan) at the PNF^2 – CNRS platform in Toulouse. Active material films previously prepared were cut into disks of 16 mm diameter and placed into a 15-mm inner diameter carbon cylindrical die (see Fig. 1). A pulse configuration of 12 pulses (one pulse duration 3.3 ms) followed by 2 periods rest (zero current) (6.6 ms) of was used to directly heat the die by Joule effect. The temperature was monitored and measured using a thermocouple inserted at the surface of the die through a small hole. A heating rate of 100 °C min^{-1} was used to reach a final temperature of 1000 °C. An uniaxial pressure of 25 MPa was applied for 1 min as soon as the dwell temperature was reached. The cooling rate was 100 °C min^{-1}. Once the thermal treatment achieved, the uniaxial pressure was gradually released within 5 min. In these conditions, during the sintering cycle, the current passing through the die and the voltage reached maximum values of 1300 A and 4.2 V, respectively.

Four different powder compositions were tested by varying the activated carbon/PTFE ratio (5, 10, 15 and 50 wt% of PTFE).

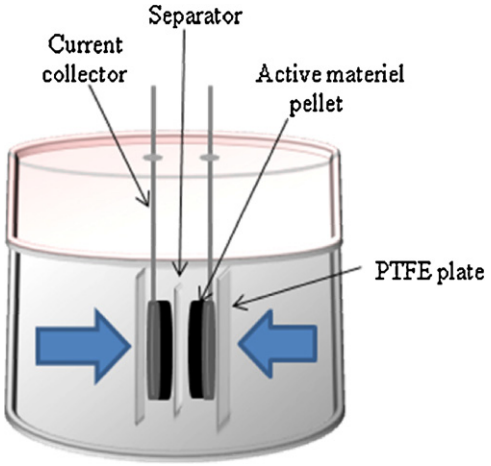

Fig. 2. Sketch of the two-electrode cell stack.

2.2. Gas sorption measurements

Gas sorption isotherm was recorded using an ASAP 2020 Micromeritics equipment using Ar gas at the liquid nitrogen temperature. Calculations of the Specific Surface Area (SSA) were achieved using the Brunauer–Emmet–Teller (BET) equation. Pore size distributions and mean pore size were calculated using the DFT and Monte-Carlo methods, according to the procedure described by Dash et al. [21].

2.3. SEM

SEM observations of the various pellets were made using a FEG-SEM (Jeol JSM 6700F).

2.4. Cell assembly

Cells were assembled in a glove box (under Ar 6.0 atmosphere) with both water and oxygen content lower than 1 ppm. Electrodes were prepared by pressing the sintered active material films on treated Aluminum current collectors [20]. Two-electrode stacks were assembled by inserting a 50 μm-thick porous polymeric separator between the two electrodes; two PTFE plates and two stainless steel clamps were placed to press the stack. The stack (Fig. 2) was immersed in a 1.5 M NEt_4BF_4 dried salt dissolved in acetonitrile (AN, <10 ppm water) electrolyte.

2.5. Electrochemical measurements

Electrochemical Impedance Spectroscopy (EIS) measurements were done with a PARSTAT 2273 apparatus (Biologic equipment). A sinusoidal voltage ($\Delta V = \pm 10$ mV) was applied, for frequencies ranging from 50 kHz to10 mHz, at a bias voltage of 0 V.

Galvanostatic cycling experiments were performed using a BT2000 Arbin cycler between 0 and 2.3 V, at various current densities (5 and 50 mA cm^{-2}).

3. Results and discussion

3.1. Spark plasma sintering of the activated carbon – PTFE (AC-PTFE) composite electrodes

In the films, before sintering, the activated carbon particles are bounded together by the PTFE fibrils, maintaining the grains in close contact. During the sintering process, the PTFE fibrils are carbonized and transformed into carbon (pyrolized polymer), while

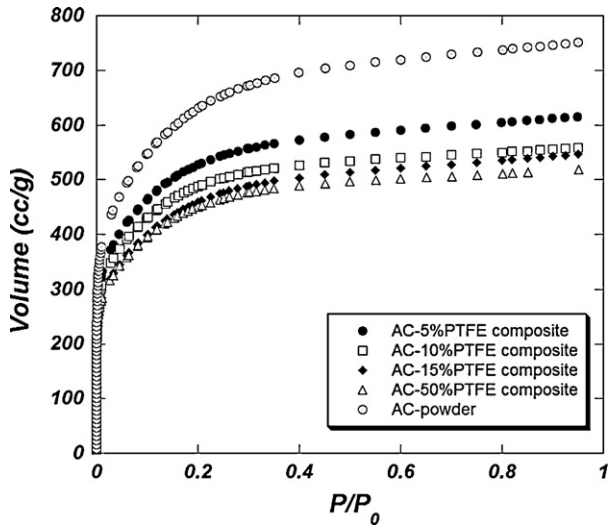

Fig. 3. Adsorption isotherms of powder and sintered activated carbon-PTFE electrodes prepared by SPS.

the fluorine are removed through HF gassing. These pyrolized polymer chains fibers contribute to the strengthening of the mechanical properties of the electrodes bring by the flash sintering process.

Self-supported composite electrodes of 15 mm diameter and 600 μm thick were reproducibly obtained.

After sintering, the porous composite Activated Carbon – PTFE electrodes were characterized using – gas sorption techniques to characterize the influence of the sintering process onto the porous structure of the electrodes.

3.2. Gas sorption measurements

All the adsorption isotherms (Fig. 3) are typical from of microporous carbons (type 1), with a plateau associated with the saturation of the adsorbent, when increasing the pressure.

The calculated Specific Surface Area (SSA), micro- and mesoporous volumes as well as mean pore size are listed in Table 1.

The raw activated carbon powder shows a surface area of 2000 $m^2 g^{-1}$, with a mean pore size of 1.1 nm, which was previously found suitable for a use as an active material in EDLC in the 1.5 M NEt_4BF_4 electrolyte [22]. From Table 1, it can be seen that increasing the PTFE content leads to a decrease of the specific area of the AC-PTFE composite electrodes. In the same way, the porous volume (micro- and mesoporous) decreases with the increase of PTFE content, while the percentages of microporous and mesoporous volumes were kept roughly the same. This can be explained by the decrease of the high surface area activated carbon content in the electrode. However, since the pore size distribution (PSD) is an intrinsic property of the activated carbon, no major change in the PSD was expected between the various samples, which is confirmed by the results (see Table 1 and Fig. 4 PSD). The SPS allowed to prepare self-supported electrodes from porous activated carbon without affecting the physical properties of the active material.

3.3. SEM observations

Fig. 5a shows the SEM picture of an activated carbon film prepared from the conventional route, with activated carbon particles bound together with the PTFE binder form. This conventional film preparation route consists in mixing the activated carbon powder with 5% PTFE in ethanol to prepare an ink. After slow removal of the ethanol by heating at 80 °C, the obtained paste is calendered onto a glass substrate to obtain the activated carbon film [21]. Fig. 5b shows the sintered activated carbon pellet containing 15% of PTFE binder. The comparison of the two pictures shows the difference in density of the two electrodes, with the carbon particles densely packed together for the sintered pellet (6b) and the low-density calendered film. Electrode density has been measured by dividing the electrode weight by its volume; densities of 0.75 and 0.4 g cm^{-3} were calculated respectively for the sintered and conventional electrodes.

3.4. Electrochemical characterization of thick (600 μm) electrodes

Galvanostatic cycling experiments were performed at a constant current density of ±5 mA cm^{-2}, between 0 and 2.3 V for 10 cycles, to measure the initial capacitance and resistance of the cells assembled with the sintered electrodes. The results obtained for the various compositions are reported in Table 2. Capacitance and resistance values of a cell assembled with 95%AC-5%PTFE films prepared using the conventional wet route – i.e. dispersing the powders into alcohol solution to form and ink [20,23] and rolling the paste until formation of a film – are given for comparison purpose.

For SPS-prepared electrodes, the specific capacitance increases with PTFE addition up to reach a maximum for 15% of PTFE. As suggested previously, PTFE is thought to improve the mechanical properties of the electrodes by bridging the carbon grains with pyrolyzed PTFE. There is then a minimum content of PTFE needed to observe an increase of the mechanical properties of the sintered electrode. On the other hand, PTFE has to be considered as a dead weight from the capacitance point of view since the contribution of the pyrolyzed PTFE to the capacitance was found to be negligible. Accordingly, an increase of the PTFE content beyond an optimum value would lead to a decrease of the electrode specific capacitance. Additionally, for high PTFE content, a part of the pores might be blocked by the carbon deposit.

This is what is typically observed in Table 2. The minimum content of PTFE seems to be around 15% to exploit the full capacitance of the carbon electrode; beyond this value, the capacitance is decreased since the PTFE dead weight in the electrode is too high and might hamper the ion accessibility into the pores. The capacitance reaches 110 F g^{-1} for the 15% PTFE sample, which is at least comparable to the reference (film) electrodes, obtained using the conventional wet route.

Electrochemical Impedance Spectroscopy (EIS) measurements were then performed to characterize the frequency behavior of the cells as well as the contribution of the ionic resistance inside the porous electrodes to the cell impedance. Fig. 6 shows the Nyquist

Table 1
BET SSA, porous volumes and pore size of the sintered activated carbon-PTFE electrodes prepared by SPS.

	AC powder	AC-5%PTFE	AC-10%PTFE	AC-15%PTFE	AC-50%PTFE
BET surface (m^2/g)	1990 (±10)	1650	1530	1450	1420
Microporous volume ($cm^3 g^{-1}$)	0.659 (77%)	0.567 (80%)	0.524 (82%)	0.484 (78%)	0.478 (80%)
Mesoporous volume ($cm^3 g^{-1}$)	0.200 (23%)	0.136 (20%)	0.116 (18%)	0.136 (22%)	0.114 (20%)
Mean pore size (nm)[a]	1.11	1.05	1.02	1.07	1.05

[a] 85% of pore volume below this size [22]. Accuracy of porous volume is 5%.

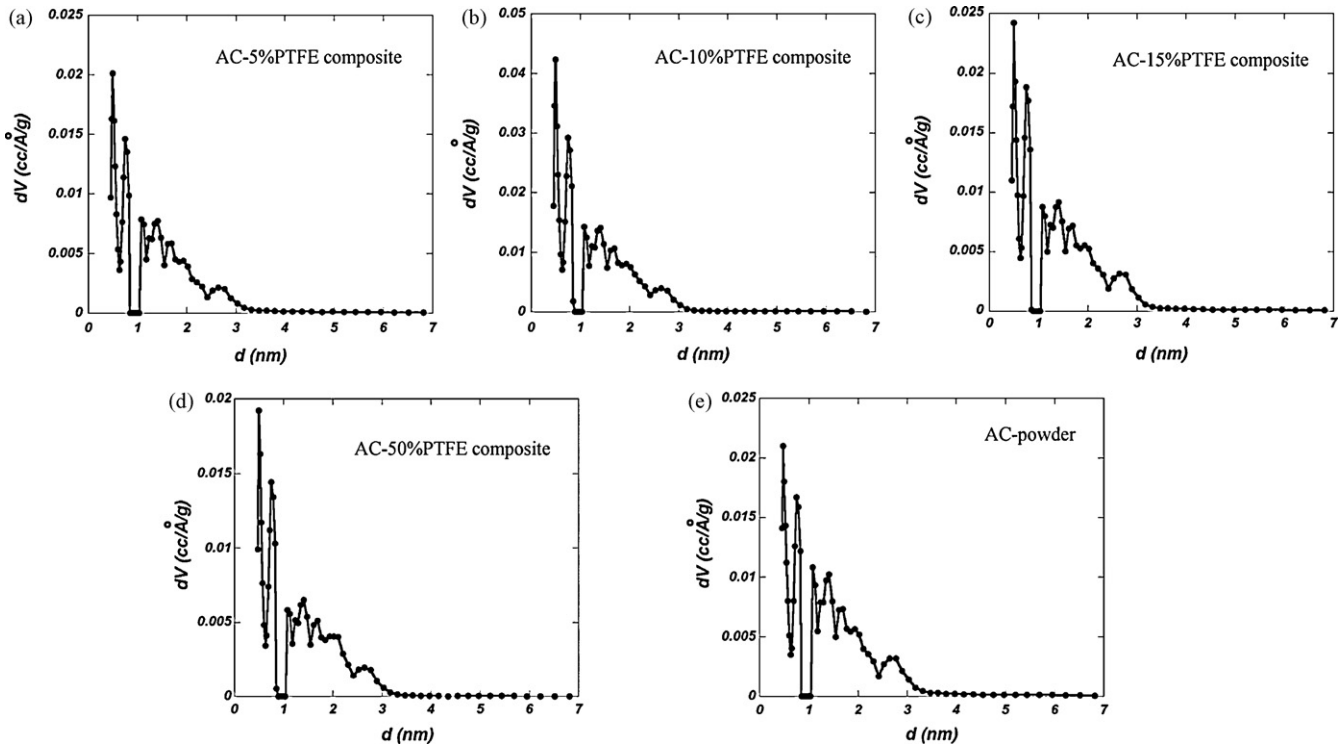

Fig. 4. PSDs of AC powder (e) and various CA-PTFE composite electrodes (a–d).

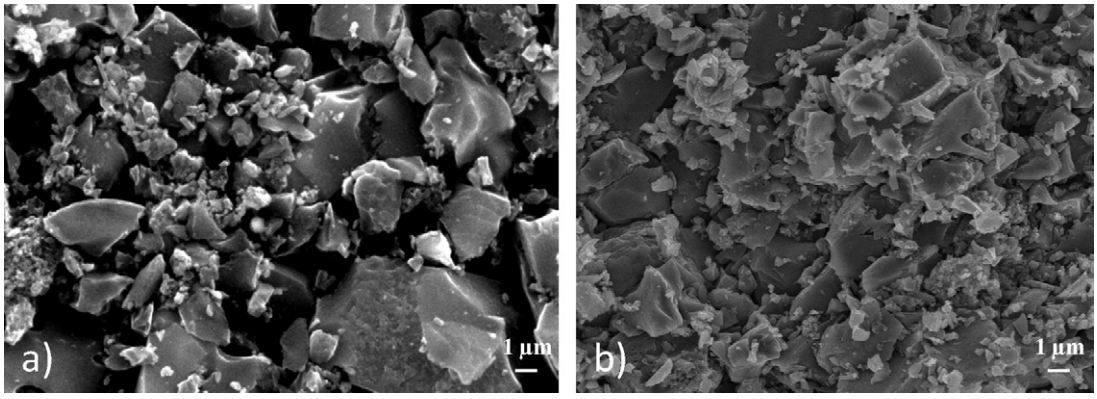

Fig. 5. FEG-SEM of an activated carbon film (a) obtained using the conventional casting route, and the composite electrodes (b) AC-15%PTFE.

Table 2
Carbon specific capacitance and cell series resistance of the cells assembled with film and SPS electrodes.

	Composition AC-PTFE	Electrode thickness (μm)	C_0 (F/g) ±2.5	R_0 @ 1 kHz (Ω cm^2) ±0.01
Film (conventional wet route [20,23])	AC-5%	300	105	0.55
SPS-prepared electrodes	AC-5%	600	76	0.48
	AC-10%	600	91	0.48
	AC-15%	600	110	0.47
	AC-50%	600	79	0.55

plots at a bias voltage of 0 V of the cells assembled using sintered electrodes (a) and conventional electrodes used as reference (b).

Whatever the PTFE content in the sintered electrodes, all the samples exhibit the same trend characteristic of a capacitive double layer behavior [23] as can be seen in Fig. 6a. At high-frequency (>1 kHz), the imaginary part of the Nyquist plot is null and the real part of the impedance is call the cell Equivalent Series Resistance (ESR). The ESR of the 15% PTFE cell was 0.5 Ω cm^2 (Table 2). The high-frequency resistance is the sum of the contribution of the bulk electrolyte resistance as well as the electrical resistance of the electrode, the latter containing the contributions of the carbon resistance, carbon/carbon contact resistance and the carbon film/current collector resistance. No high-frequency loop was observed on any Nyquist plot, thus demonstrating that the carbon film/current collector contact impedance was small [20].

More interesting, this high-frequency resistance was found to be in the same range – even slightly lower – than that of the reference cell assembled with rolled films in the same conditions (same separator and electrolyte) [20,23]. However, in the present work,

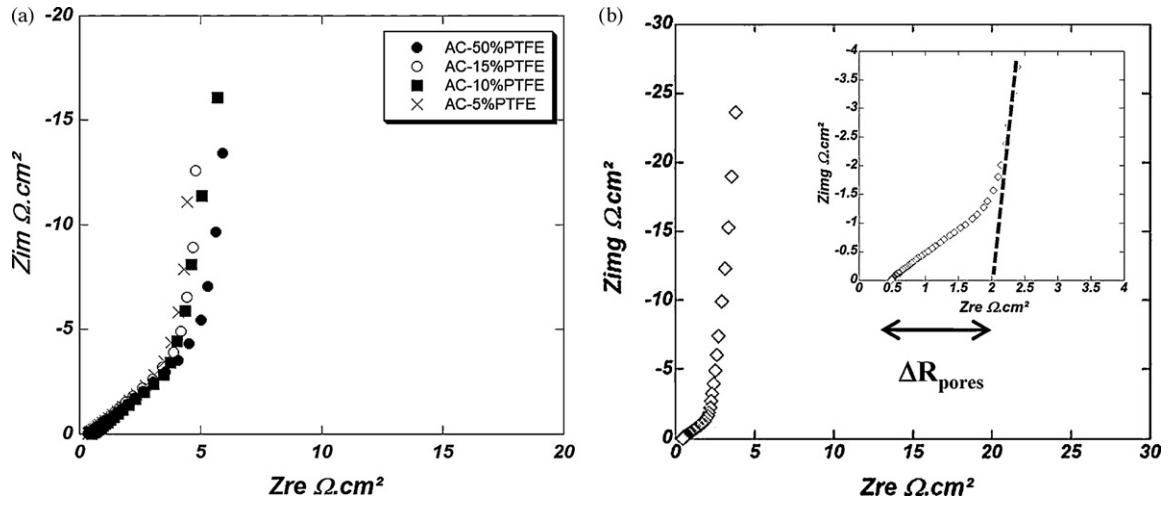

Fig. 6. Nyquist plots of SPS cell (a), of standard cell – AC-5%PTFE (b). Inset: determination of the ionic resistance of the electrolyte inside the porous carbon ΔR_{pores}.

the thickness of the sintered electrodes is twice than that of rolled electrodes (600 μm vs 300 μm). Accordingly, the improvement of the electrical resistance of the electrode is one of the interests of the SPS technique for designing high power devices.

At very low frequency (<10 mHz), the quasi-vertical line observed in Fig. 6 shows the capacitive behavior of the system. The transition between these two regimes, indicated by a linear Warburg-like behavior, originates from the porous network of the activated carbon [23,24]. This region corresponds to the penetration of the electrolyte into the porous structure of the electrode. Once the total capacity of electrode is reached, the imaginary part sharply increases [23,25]. The difference between the high-frequency resistance (ESR) and the extrapolation of the low frequency linear capacitive behavior on the real part axis defines the electrolyte resistance inside the carbon porous network ΔR_{pores} (see Fig. 6b).

For cells assembled with sintered electrodes, the ionic resistance of the electrode ΔR_{pores} is about 4 Ω cm^2 (Fig. 6a), which is very high when compared to the cell using rolled electrodes (1.5 Ω cm^2, see Fig. 6b). This higher ionic resistance certainly comes from the higher thickness of sintered electrodes (600 μm), thus hampering the power capability of the device. Following these results, thinner sintered electrodes (300 μm-thick) were prepared with the composition showing the best electrochemical performances (85%AC-15%PTFE).

Fig. 7a shows the galvanostatic cycling at ±5 mA cm^{-2} between 0 and 2.3 V and Fig. 7b shows the Nyquist plot of a two-electrode cell assembled with 300 μm-thick sintered electrodes.

The cycling behavior (Fig. 7a) was found to be linear within the voltage window studied, demonstrating the absence of any parasitic faradic reaction. A capacitance of 95 F g^{-1} was measured, which was close to that of the reference conventional electrode cell (105 F g^{-1}, see Table 1). This is assumed to be linked with the higher compaction rate observed (88% and 72%, respectively for 300 and 600 μm, respectively). Accordingly, the thinner electrodes offer an accessible area slightly reduced to the ions of the electrolyte, resulting in a small capacitance loss (<10%).

The impedance spectroscopy plot (Fig. 7b) shows again a typical capacitive behavior with the different regions previously described above. However, the ionic resistance of the cell was measured at about 3 Ω cm^2, which is less than that of the thicker electrodes is prepared in the present study. Although this was an expected result – decreasing the electrode thickness decrease the ionic resistance – this results is interesting since it demonstrates that consolidate electrodes can be prepared using the SPS techniques with similar performance than that of electrodes prepared using the conventional route.

Cycling stability of the cell was also checked. Fig. 8 shows the change of the ESR and capacitance over 10,000 cycles. The capacitance loss is about 10% during the first 4000 cycles and remains

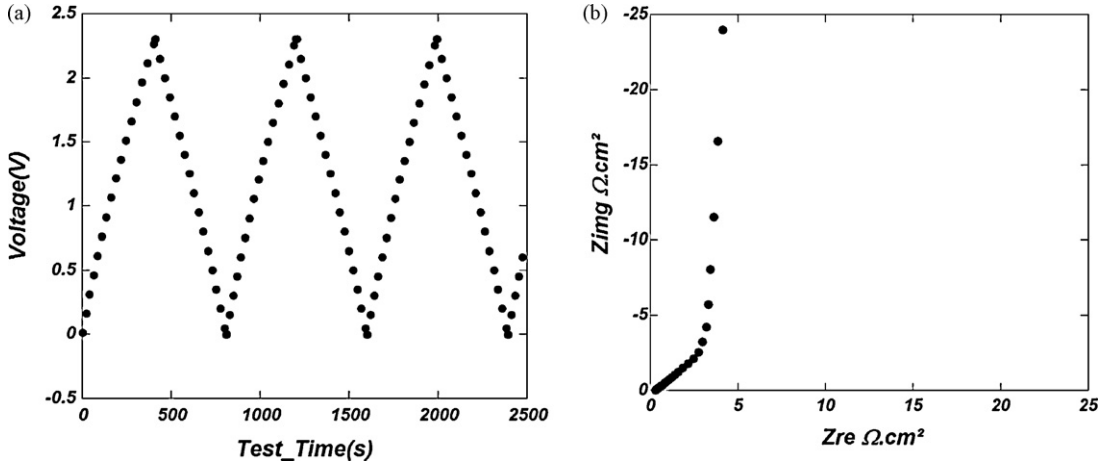

Fig. 7. Initial performances of 300 μm electrode AC-15%PTFE; (a) galvanostatic cycling between 0 and 2.3 V at ±5 mA cm^{-2} and (b) Nyquist plot of the cell at a bias voltage of 0 V.

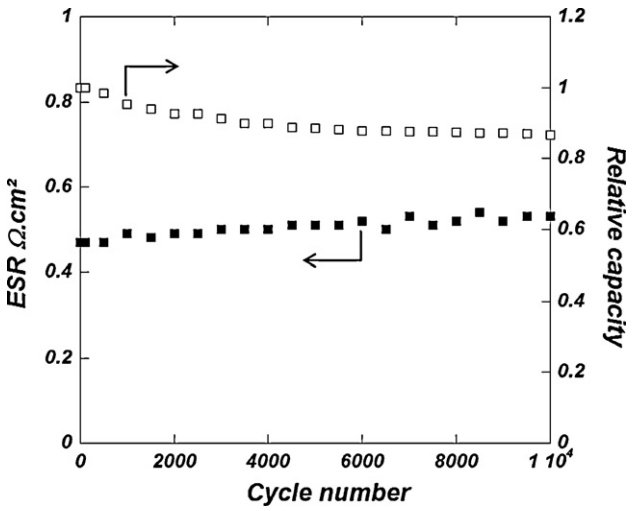

Fig. 8. Relative capacity and ESR changes for the two-electrode cell assembled with the 300 μm-thick composite electrodes AC-15%PTFE sintered electrodes.

constant during the subsequent 5000 cycles. The cell series resistance (measured at 20 Hz during cycling) is only increased by 10% during the first 6000 cycles and then is kept constant at 0.55 Ω cm^2, which is a value compatible with high power performance expected from supercapacitor systems.

These results show that the SPS technique can be successfully used to prepare sintered electrodes with electrochemical performance close to classical tape-casted or rolled electrodes. This is really interesting since it opens new paths for designing solid-state supercapacitors that could be processed in one-step by sandwiching a porous insulating ceramic powder like Al_2O_3 between two carbon electrodes. This work is currently under progress at the lab.

4. Conclusion

This paper shows the first results of the use of the SPS technique to prepare sintered porous carbon electrodes, with the final goal to design a solid-state supercapacitor device.

Self-supported activated carbon pellets of 15 mm diameter were prepared by heating directly the samples by Joule effect under pressure; a heating rate of 100 °C min^{-1} was used to reach a final temperature of 1000 °C under 25 MPa. The porous structure of the activated carbon pellets was not affected by the flash sintering treatment and the pore size distribution was kept the same for the raw activated carbon powder. Electrochemical characterization of a two-electrode cell assembled with 300 μm-thick sintered activated carbon pellets have shown a typical capacitive behavior in acetonitrile-based electrolyte, with a gravimetric capacitance of 95 F g^{-1} and a series resistance 0.5 Ω cm^2. These values were comparable to the performance of conventional electrodes prepared from a mixture of activated carbon and binder. Galvanostatic cycles showed excellent capacitance retention (−15%) and only 10% increase in the series resistance, most of the variation occurring during the first 5000 cycles.

These first electrochemical results clearly demonstrate that the SPS technique is suitable for preparing supercapacitor electrodes and this validates the first towards the design of an all solid-state supercapacitor.

References

[1] B.E. Conway, Electrochemical Capacitor: Scientific: Fundamentals and Technological applications, Plenum Press, New York, 1999, p. 545.
[2] P. Simon, Y. Gogotsi, Nature Materials 7 (2008) 845–854.
[3] R. Kötz, M. Carlen, Electrochimica Acta 45 (2000) 2483.
[4] R. John, Science 321 (2008) 651–652.
[5] K.C. Chen, H.T. Li, T. Nemoto, S.C. Huang, T. Fukui, T.M. Lee, K. Kitamura, T. Tsuji, Book series: IEEE 29th International Electronics Manufacturing Technology Symposium, 2004, pp. 119–123.
[6] M. Tokita, Journal of the Society of Powder Technology Japan 30 (11) (1993) 790–804.
[7] K. Inoue, US Patent, No. 3 250 892 (1966).
[8] J.X. Zhang, Q.M. Lu, K.G. Lui, L. Zhang, M.L. Zhou, Materials Letters 58 (2004) 1981–1984.
[9] C.Y. Xü, S.S. Jia, Z.Y. Cao, Materials Characterization 54 (2005) 394.
[10] J.R. Groza, S.H. Risbud, K. Yamazaki, Journal of Materials Research 7 (1992) 2643.
[11] R. Chaim, Z. Shen, M. Nygren, Journal of Materials Research 19 (2007) 2527.
[12] Z. Song, S. Kishimoto, N. Shinya, Journal of Materials Science 38 (2003) 4211–4219.
[13] J. Gurt Santanach, C. Estournès, A. Weibel, A. Peigney, G. Chevallier, Ch. Laurent, Scripta Materiala 60 (2009) 195–198.
[14] C. Estournès, Shaping materials by flash sintering. Techniques de l'Ingénieur, Matériaux Métalliques (2006) 48(M 187), IN56/1-IN56/8.
[15] Y. Kobayashi, T. Takeuchi, M. Tabuchi, et al., Journal of Power Sources 81 (1999) 853–858.
[16] Y. Kobayashi, H. Miyashiro, T. Takeuchi, H. Shigemura, N. Balakrishnan, M. Tabuchi, H. Kageyama, T. Iwahori, Solid State Ionics 152 (2002) 137–142.
[17] J. Galy, M. Dolle, T. Hungria, P. Rozier, J.-Ph. Monchoux, Solid State Sciences 10 (2008) 976–981.
[18] S. Guillemet-Fritsch, Z. Valdez-Nava, C. Tenailleau, T. Lebey, B. Durand, J.Y. Chane-Ching, Advanced Materials 20 (2008) 551–555.
[19] U.C. Chung, C. Elissalde, S. Mornet, M. Maglione, C. Estournès, Applied Physics Letters 94 (2009).
[20] C. Portet, P.L. Taberna, P. Simon, C. Laberty-Robert, Electrochimica Acta 49 (2004) 905–912.
[21] R. Dash, J. Chmiola, G. Yushin, Y. Gogotsi, G. Laudisio, J. Singer, J. Fischer, S. Kucheyev, Carbon 44 (2006) 2489–2497.
[22] J. Chmiola, G. Yushin, C. Portet, P. Simon, P.L. Taberna, Science 313 (2006) 1760–1763.
[23] P.L. Taberna, P. Simon, J.F. Fauvarque, Journal of the Electrochemical Society 150 (2003) A292.
[24] C. Portet, P.L. Taberna, P. Simon, E. Flahaut, C. Laberty-Robert, Electrochimica Acta 50 (2005) 4147–4181.
[25] R. de Levie, Electrochimica Acta 9 (1964) 1231.